

Enhancing Aircraft Performance Through Flight/Propulsion System Integration

By

P. K. Menon* and V. R. Iragavarapu[†]

Optimal Synthesis

Palo Alto, CA

Sanjay Garg[‡]

NASA Lewis Research Center

Cleveland, OH

Abstract

Aircraft performance enhancement by integrating the propulsion control system with the primary flight control system is demonstrated through two nonlinear flight control design examples. In the first example, high performance aircraft turning performance improvement using engine thrust modulation is demonstrated. In the second example, the flight propulsion system integration is used to achieve precise flight time control for a transport aircraft. Both control law designs are based on feedback linearization, and exploit the aircraft dynamic models. Realistic aircraft models are used to illustrate the responses of the nonlinear integrated flight/propulsion control systems.

1. Introduction

The importance of integrated flight/propulsion control system in STOVL aircraft and in hypersonic aircraft has been clearly established in the literature [1 - 5]. The objective of the present paper is to illustrate the role of integrated flight/propulsion control technology in improving the performance and operational utility of conventional aircraft. A turn coordination autopilot for a conventional high performance aircraft, and a precision time/altitude tracking control system for a wide-body transport aircraft are developed to illustrate the benefits of the integrated flight/propulsion control (IFPC) technology.

Traditional flight control configurations consider the dynamic relationship between the engine and airframe only for the design of speed control systems [6]. Other flight control functions such as airframe stabilization and maneuver control exclusively employ aerodynamic control surfaces. The implicit assumption being that the engine thrust is either constant or slowly varying. Recent development of 2-D thrust vectoring capabilities offer the potential for an improved degree of flight/propulsion control system integration. It will be shown in the present paper that even when thrust vectoring capabilities are not available, integrating the propulsion

^{! *} Research Scientist, Associate Fellow AIAA

[†] Research Scientist, Member AIAA

[‡] Aerospace Engineer, Associate Fellow AIAA

system with primary flight control system can result in improved aircraft performance and operational utility.

Integrated flight/propulsion system control technology can add value to existing aircraft incorporating traditional flight control systems without significant increase in cost. This represents a large retrofit market for both high performance aircraft and large transport aircraft. However, due to the additional level of complexity it introduces in the flight control system, the benefits of IFPC technology has to be clearly demonstrated before it becomes more widely acceptable to the flight controls community. The following sections will discuss the motivation for integrating the flight control system with the propulsion control system, and will present the development of nonlinear controllers.

2. High Performance Aircraft Turn Rate Improvement

A large class of air combat engagements can be considered to consist of two basic maneuvers: turns followed by dash [7]. The turn maneuver is used to orient the aircraft velocity vector in a desired direction, while the dash maneuver involves accelerating at the maximum rate to achieve the maximum speed. In order to exploit all the capabilities of an aircraft, both these maneuvers will need to be optimized during air combat. Dash maneuver usually involves flight at maximum afterburner power to reach the maximum speed point on the flight envelope. Although altitude transitions are a part of the dash maneuver, thrust is seldom modulated.

However, in conventional as well as in high angle of attack flight, optimum aircraft turn maneuver is known to involve significant thrust modulation [8]. A simple analysis presented in following will reveal this fact. The turn rate of an aircraft with its thrust vector closely aligned with the velocity vector, and under coordinated flight is given by the expression [7]:

$$\dot{\chi} = \frac{L \sin \mu}{mV \cos \gamma}$$

Here, $\dot{\chi}$ is the turn rate, χ is the heading angle, L is the aircraft lift, m the mass, V is the airspeed, γ is the flight path angle and μ is the bank angle.

Examining the right hand side of the $\dot{\chi}$ equation shows that for a given load factor L/mg , the turn rate can be increased by decreasing the aircraft speed during the turn, or by changing the flight path angle towards ± 90 degrees. Most modern fighter aircraft are capable to delivering higher load factors than the human pilot can tolerate. Hence, in g-limited turns, the aircraft turn rate can be maximized only by actively controlling the airspeed. Airspeed control can be

accomplished by varying the engine thrust during maneuvers. Note this development assumes the capability for a rather rapid thrust modulation.

In the cases where the altitude can also change during the turn, it is more appropriate to examine the turn rate - airspeed diagram used in aircraft performance calculations. This chart is often called the corner velocity chart. A sample corner velocity chart for a high performance aircraft at a specified energy level is shown in Figure 1. This figure depicts the maximum sustainable turn rate that can be delivered by an aircraft as a function of airspeed.

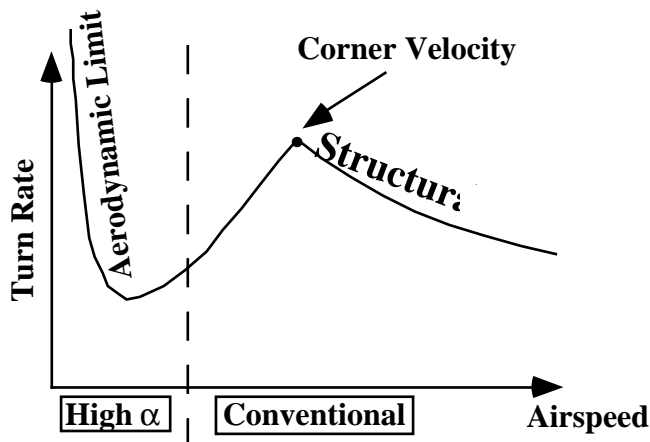


Fig. 1. Corner Velocity Diagram for a High Performance Aircraft

This diagram is characterized by two constraints: the aerodynamic or the stall constraint, and the structural limit. Corner velocity is the point of intersection of these two constraints. Corner velocity defines the speed at which maximum sustainable turn rate is achieved. Thus, if a conventional high performance aircraft desires to execute the fastest turn possible, the first step is to change the aircraft speed to the corner velocity. If the aircraft speed is higher than the corner velocity, thrust can be reduced and speed brakes can be used to bring the aircraft speed to the corner velocity. On the other hand, if the aircraft speed is slower than the corner velocity, thrust increase can be used to improve aircraft turn rate.

In the high angle of attack regime, the aircraft speed is reduced to a low value by pulling up the nose, cutting the throttle, and executing the turn at the lowest possible airspeed. Immediately after this maneuver, since the aircraft is rapidly losing energy, full afterburner thrust is employed to ensure a graceful recovery.

Once the aircraft has completed its turn, it normally transitions onto a dash maneuver, requiring full afterburner power. From the following discussions, it is clear that simultaneous control of airframe and propulsion system will be extremely beneficial in improving the turn performance of high performance aircraft.



These facts have been known for some time. However, they have not been exploited to modify the turn coordination autopilots used in high performance aircraft. In the following, a high performance aircraft model will be used to develop a turn coordination autopilot that employs thrust modulation to improve the turn rate. The effect of varying the level of flight/propulsion control integration will be demonstrated by changing the interconnection gain between the turn coordination autopilot and the propulsion control subsystem.

2.1. A-4D Aircraft Turn Rate Improvement

This study employs a horizontal plane nonlinear model of the Navy/McDonnell Douglas A-4D Skyhawk aircraft. The aircraft aerodynamic data was obtained from References 9 and 10. Since detailed engine data was not available in these references, published engine thrust data of the F-4 aircraft [11] was scaled to match the thrust to weight ratio of the A-4D aircraft. The engine thrust is given as a numerical function of altitude and Mach number. The closed-loop engine dynamics is represented by a first-order lag with a 1 second time constant.

The flight/propulsion control system integration is demonstrated by first designing a turn coordination autopilot together with an autothrottle speed control system, and then introducing a simple interconnect logic between the two control systems. Figure 2 shows the block diagram of the proposed control configuration.

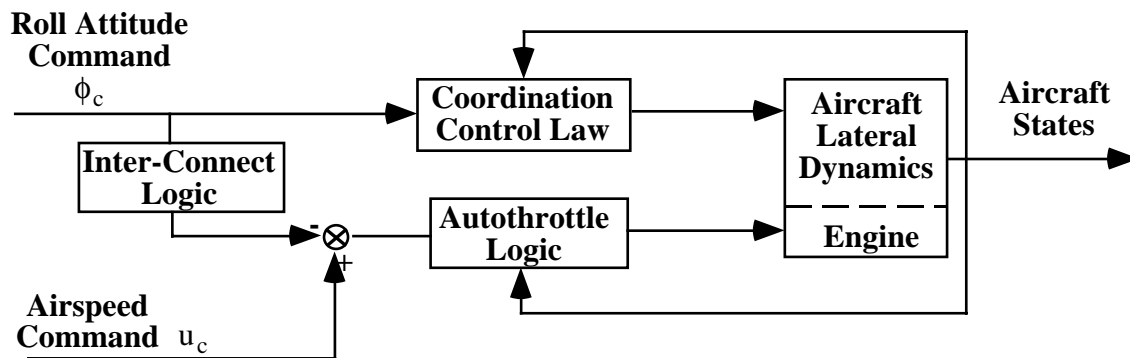


Fig. 2. Lateral Flight Control System with the Inter-Connect Logic

The pilot commands to the system are the roll attitude and airspeed setting. Note that it is not difficult to reconfigure this system to track roll rate command as in certain operational fighter aircraft. The functions of the coordination control law are to track the commanded roll attitude while maintaining the angle of sideslip near zero. Sideslip regulation is accomplished by generating an appropriate yaw rate in response to the angle of sideslip feedback. The autothrottle logic is used to track the commanded airspeed during the aircraft operation. The interconnect logic introduced between these control loops generates a speed perturbation in response to a roll

attitude command. As currently configured, a negative speed perturbation command is generated for any non-zero roll command. A very simple interconnect logic is used in the present study, as will be described subsequently in this subsection.

The flight control system design is based on the aircraft equations of motion in the horizontal plane given in the following. These equations can be obtained by setting the vertical velocity and pitch rate to zero, together with force equilibrium in the vertical plane, and moment equilibrium about the pitch axis.

$$\begin{aligned}\dot{u} &= a_x + r \quad v \\ \dot{v} &= a_y + g \sin \phi - r \quad u \\ \dot{p} &= \frac{I_z}{I_x I_z - I_{xz}^2} l + \frac{I_{xz}}{I_x I_z - I_{xz}^2} n \\ \dot{r} &= \frac{I_{xz}}{I_x I_z - I_{xz}^2} l + \frac{I_x}{I_x I_z - I_{xz}^2} n \\ \dot{\phi} &= p \\ \dot{\chi} &= \frac{g}{\sqrt{u^2 + v^2}} \tan \phi \\ \dot{x} &= \sqrt{u^2 + v^2} \cos \chi \\ \dot{y} &= \sqrt{u^2 + v^2} \sin \chi\end{aligned}$$

In these equations, u and v are the aircraft body velocity components along the longitudinal and lateral directions. The longitudinal and lateral acceleration components are given by :

$$a_x = \frac{(\eta T_{\max} - D)}{m} \quad \text{and} \quad a_y = \frac{(C_{y\beta} \beta + C_{y\delta_a} \delta_a) \bar{q} s}{m}$$

The variables p , r are the roll and yaw body rates. The variables I_x and I_z are the aircraft moment of inertia components, and I_{xz} is the product of inertia. These equations assume that the aircraft configuration is symmetric about the vertical plane. The roll moment is denoted by the variable l , and the yaw moment is denoted by the variable n . The variable ϕ is the roll attitude, χ is the heading angle and η is the throttle setting. The variable x denotes the down range and y is the cross range. The drag D and the lift L lift are calculated using the expressions:

$$D = \bar{q} s (C_{D\alpha} |\alpha|), \quad L = \bar{q} s C_{L\alpha} \alpha$$

The rolling moment l and the yawing moment n are defined as:

$$\begin{aligned}l &= \bar{q} s b \left(C_{l\beta} \beta + C_{l_p} \frac{b}{2V_T} p + C_{l_r} \frac{b}{2V_T} r + C_{l\delta_a} \delta_a + C_{l\delta_r} \delta_r \right) \\ n &= \bar{q} s b \left(C_{n\beta} \beta + C_{n_p} \frac{b}{2V_T} p + C_{n_r} \frac{b}{2V_T} r + C_{n\delta_a} \delta_a + C_{n\delta_r} \delta_r \right)\end{aligned}$$

The dynamic pressure is computed using the expression : $\bar{q} = \frac{1}{2} \rho V_T^2$.

In order to avoid dealing with extensive gain scheduling, both the coordination control law and the autothrottle logic are synthesized using the feedback linearization technique [12 - 15]. The synthesis of the autothrottle logic using feedback linearization will be illustrated first, followed by the development of the coordination control law.

Since the coordination control law will maintain the lateral velocity near zero, the speed control system design can be based solely upon the differential equation for longitudinal velocity. The first step in the control law design is to set the right hand side of the longitudinal velocity equation to a pseudo-control variable U_1 . This process can be interpreted as a transformation that converts the original nonlinear dynamic system into a linear time-invariant form. In this case, the longitudinal velocity equation will be of the form:

$$\dot{u} = U_1$$

This equation is in linear time-invariant form with respect to the pseudo-control variable and a linear control law can be designed to track the commanded velocity profile. Since the speed control law may be required to track ramp airspeed commands, good tracking response can be achieved by using a proportional plus integral control law. Thus, the control law in terms of the pseudo-control variable will be of the form:

$$U_1 = k_1(u_c - u) + k_2 \int_0^t (u_c - u) dt$$

The proportional and integral gains can be chosen to yield any desired control law bandwidth. The feedback gains used in the present research are $k_1 = 2$ and $k_2 = 1$. Next, if one assumes that all the state variables are available as measurements, and if a reasonably good approximation of the maximum engine thrust model and aerodynamic coefficients are available, the throttle setting required to track a commanded longitudinal velocity can be obtained by equating the above expression to the right hand side of the longitudinal velocity equation. This process can be considered to be an inverse transformation of the system nonlinearities. The inverse transformation of the pseudo-control law yields:

$$\eta = \frac{D}{T_{\max}} + \frac{m}{T_{\max}} \left[\left\{ k_1(u_c - u) + k_2 \int_0^t (u_c - u) dt \right\} - r v \right]$$

The speed control system configuration resulting from the foregoing analysis is illustrated in Figure 3. In addition to the longitudinal velocity, the control law requires an internal estimate of the aircraft drag, mass, and maximum thrust. Additionally, the lateral velocity and the yaw rate are also required to complete the control computations.

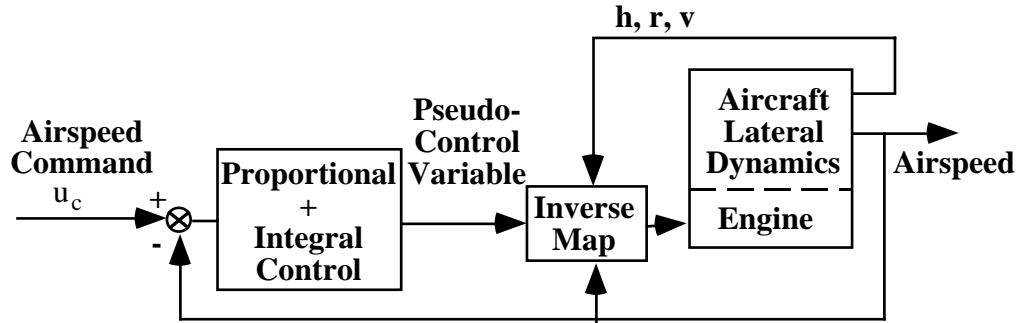


Fig. 3. Airspeed Control System

The design of roll/yaw controller proceeds in a similar fashion. The roll attitude equation is differentiated once with respect to time, and the differential equation for roll rate is used to eliminate the variable $\dot{\phi}$ to yield:

$$\ddot{\phi} = \frac{I_z}{I_x I_z - I_{xz}^2} l + \frac{I_{xz}}{I_x I_z - I_{xz}^2} n$$

This differential equation can be feedback linearized by setting the right hand side to a pseudo-control variable. This yields a linear, time-invariant dynamical system of the form:

$$\ddot{\phi} = U_2$$

A proportional plus derivative control law can be designed for this system to track commanded roll attitude as:

$$U_2 = k_3 (\phi_c - \phi) - k_4 \dot{\phi}$$

The feedback gains can be chosen to obtain any desired time response. For the present study, the gains used were $k_3 = 39.44$ and $k_4 = 8.88$. These correspond to an undamped natural frequency of 2 Hz and a damping coefficient of 0.707. The actual control variables can be recovered by equating the right hand side of the original roll angular acceleration equation to the pseudo-control variable to yield:

$$k_3 (\phi_c - \phi) - k_4 \dot{\phi} = \frac{I_z}{I_x I_z - I_{xz}^2} l + \frac{I_{xz}}{I_x I_z - I_{xz}^2} n$$

However, since roll acceleration depends on both the roll moment and yaw moment, the actual control variable for the roll attitude cannot be recovered from this equation until the yaw moment is also computed.

The yaw moment is next computed based on the control requirements for turn coordination achieved by maintaining angle of sideslip near zero during maneuvers. The angle of sideslip can be regulated by generating a yaw rate in response to the angle of sideslip feedback. A yaw rate tracking control law can then be used to drive the angle of sideslip to zero.

Since the angle of sideslip depends directly on the lateral velocity v , regulating the lateral velocity about zero is equivalent to angle of sideslip regulation. As in the development of the autothrottle logic, the right hand side of the lateral velocity equation is first set to a pseudo-control variable to yield:

$$\dot{Y} = U_3,$$

with: $U_3 = a_y + g \sin \phi - ru$.

The transformed system is in linear, time-invariant form, and a control law of the form : $U_3 = -k_5 v$ can be used to regulate the lateral velocity about zero. Assuming the availability of all the necessary states, and a reasonably good aerodynamic model of the aircraft, the yaw rate required to maintain the lateral velocity near zero is given by:

$$r_c = \frac{1}{u} [a_y + g \sin \phi + k_5 v]$$

The feedback gain $k_5 = 2$ was used in the present case.

The control law design for tracking the commanded yaw rate similar to that followed for the other control laws developed in this section. The first step is to equate the right hand side of the yaw rate equation to a pseudo-control variable. This will yield a first-order, linear dynamic system of the form:

$$\dot{r} = U_4$$

A proportional control law of the form : $U_4 = k_6 (r_c - r)$ can be used to track the commanded yaw rate. The gain used for yaw rate tracking was $k_6 = 6.28$.

The actual control variable required to track the commanded yaw rate can be recovered by equating the right hand side of the original yaw rate equation to the pseudo control variable. Thus,

$$k_6 \left\{ \frac{1}{u} [a_y + g \sin \phi + k_5 v] - r \right\} = \frac{I_{xz}}{I_x I_z - I_{xz}^2} l + \frac{I_x}{I_x I_z - I_{xz}^2} n$$

This expression can be solved together with the expression for roll attitude control to yield the aileron/rudder deflections as:

$$\begin{bmatrix} \delta_a \\ \delta_r \end{bmatrix} = \frac{1}{(d_1 d_4 - d_2 d_3)} \begin{bmatrix} d_4 & -d_2 \\ -d_3 & d_1 \end{bmatrix} \begin{bmatrix} e_1 \\ e_2 \end{bmatrix}$$

where:

$$a_1 = \frac{I_z}{I_x I_z - I_{xz}^2}, \quad a_2 = b_1 = \frac{I_{xz}}{I_x I_z - I_{xz}^2}, \quad b_2 = \frac{I_x}{I_x I_z - I_{xz}^2}$$

$$c_1 = k_3 (\phi_c - \phi) - k_4 p, \quad c_2 = k_6 \left\{ \frac{1}{u} [a_y + g \sin \phi + k_5 v] - r \right\}$$

$$d_1 = \bar{q}sb \left(a_1 C_{l_{\delta_a}} + a_2 C_{n_{\delta_a}} \right) \quad d_2 = \bar{q}sb \left(a_1 C_{l_{\delta_r}} + a_2 C_{n_{\delta_r}} \right)$$

$$d_3 = \bar{q}sb \left(b_1 C_{l_{\delta_a}} + b_2 C_{n_{\delta_a}} \right) - \frac{k_6}{u} \left(\frac{C_{y_{\delta_a}}}{m} \bar{q} s \right), \quad d_4 = \bar{q}sb \left(b_1 C_{l_{\delta_r}} + b_2 C_{n_{\delta_r}} \right)$$

$$e_1 = c_1 - \bar{q}sb \left\{ a_1 \left(C_{l_{\beta}} \beta + C_{l_p} \frac{b}{2V_T} p + C_{l_r} \frac{b}{2V_T} r \right) + a_2 \left(C_{n_{\beta}} \beta + C_{n_p} \frac{b}{2V_T} p + C_{n_r} \frac{b}{2V_T} r \right) \right\}$$

$$e_2 = c_2 - \bar{q}sb \left\{ b_1 \left(C_{l_{\beta}} \beta + C_{l_p} \frac{b}{2V_T} p + C_{l_r} \frac{b}{2V_T} r \right) + b_2 \left(C_{n_{\beta}} \beta + C_{n_p} \frac{b}{2V_T} p + C_{n_r} \frac{b}{2V_T} r \right) \right\}$$

Figure 4 illustrates the turn coordination control system. This figure shows the sequence of computations, as well as the state variables and aircraft measurements required for feedback at every stage.

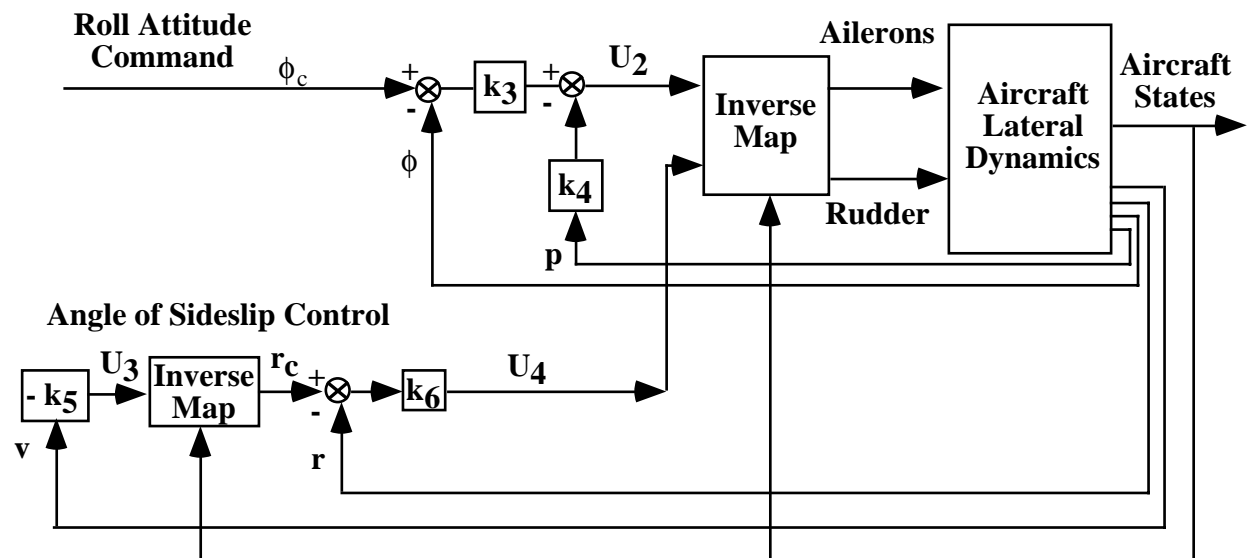


Fig. 4. Nonlinear Turn Coordination Control System

The turn coordination autopilot can next be integrated with the airspeed control system to yield the integrated flight/propulsion control system. The integration of flight and propulsion system in this application is based on the observation that in high performance aircraft, turn rate at a constant altitude can be improved by decreasing the airspeed during the turn. The lowest permissible speed is determined by the aircraft stall limit, which in turn is limited by the maximum permissible angle of attack. Thus, at a constant load factor, an improved turn maneuver can be obtained by decreasing the airspeed during the turn to the lowest permissible limit, and recovering the speed back as the aircraft completes its turn.

An interconnect logic is introduced between the automatic turn coordination autopilot and the autothrottle function to demonstrate the turn rate improvement. Due to the preliminary nature of the present study, a simple interconnect logic of the form:

$$\delta u_c = -k_t |\phi|$$

is used to investigate the effect of flight control/propulsion system integration. If the interconnection gain k_t is zero, independent autothrottle and turn coordination control functions are realized, while a non-zero interconnect gain produces the response of an integrated system. According to this interconnect logic, as the aircraft roll attitude is increased, the aircraft speed is reduced by a proportional amount. More advanced interconnect logics are possible, and these will be investigated in a future research project.

The performance of the integrated flight control system is next evaluated in a nonlinear simulation of the aircraft lateral dynamics. Although several runs have been made, only one of them will be given in this paper.

In this simulation, the aircraft is flying at an altitude of 3000m with 0.5 Mach number at the beginning of the turn maneuver. After an initial straight-line flight of 5 seconds duration, a roll angle of 60 degrees is commanded, corresponding to a load factor of 2 g's. The aircraft makes an anti-clockwise coordinated turn under this command. The roll attitude is held at 60 degrees throughout the turn maneuver. The simulation is terminated when the aircraft reaches a heading angle of 180 degrees. The turn maneuver is repeated with various interconnect gains.

Aircraft trajectories in the horizontal plane are shown in Figure 5. This figure also gives the interconnect gains and the turn maneuver durations corresponding to each value of the interconnect gain. It can be observed that as the interconnection gain is increased, the aircraft is able to reach the 180 degree heading in shorter time durations. When compared with the zero interconnect gain case, the maneuver with an interconnect gain of 40 shows a 25% improvement in the time taken to reach the final value of the heading angle. Since the load factor is maintained at a constant value of 2 g's throughout the turn maneuver, the decrease in time-to-turn is of significant practical importance.

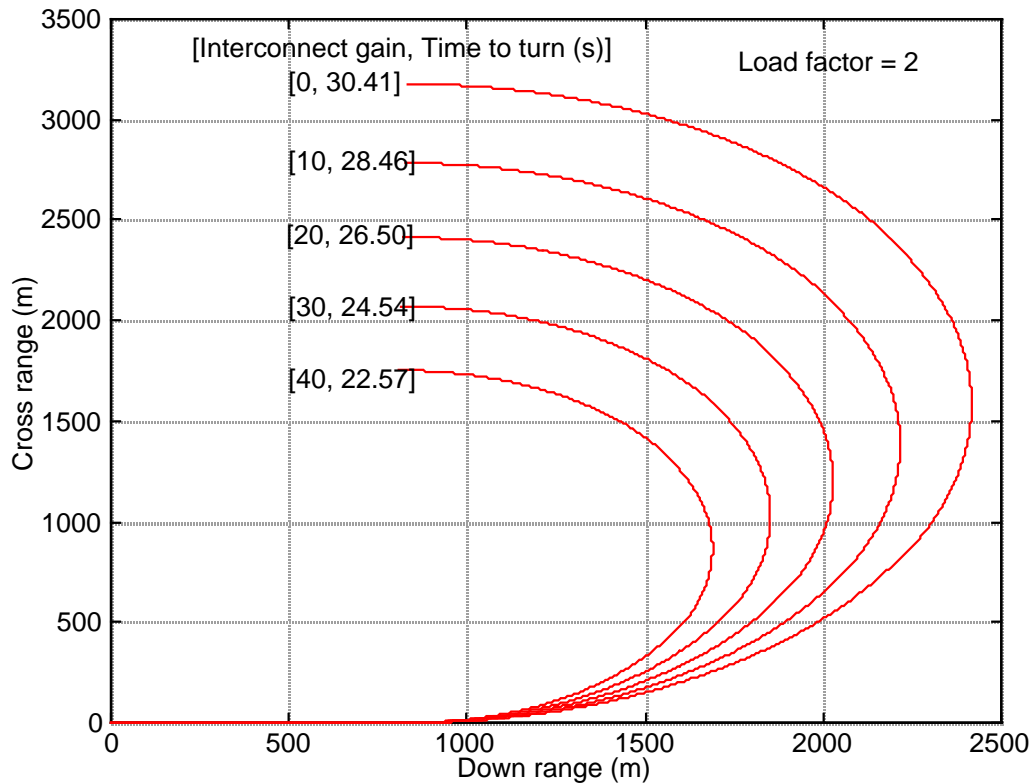
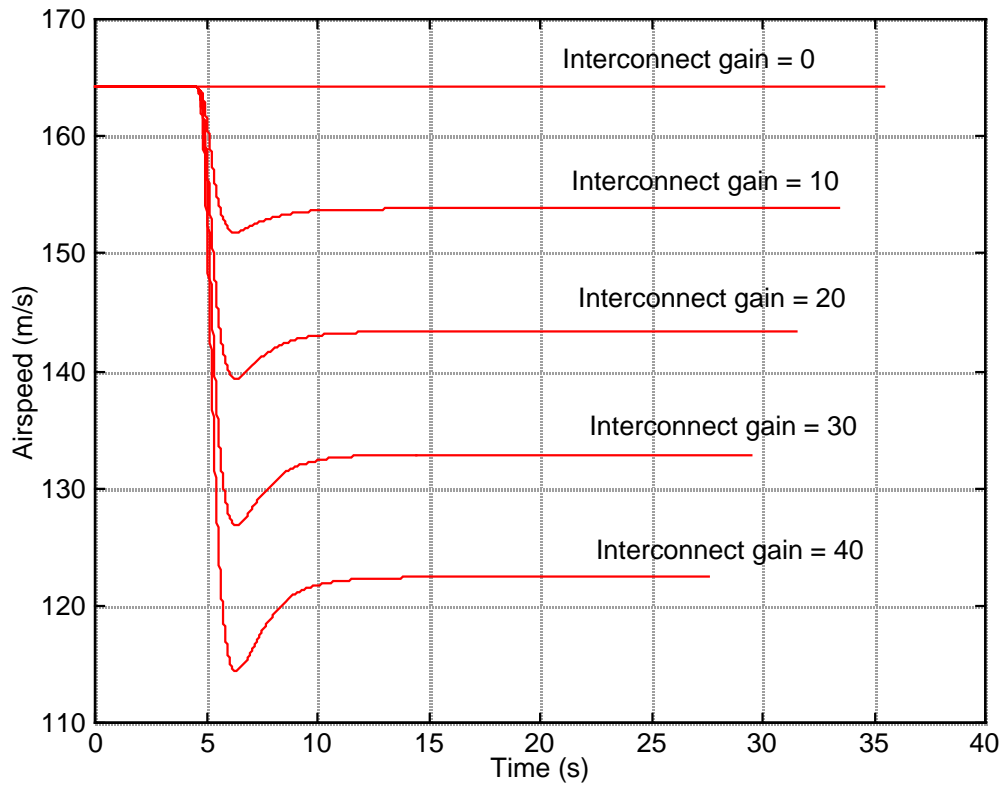


Fig. 5 Turn Performance for the A-4D Aircraft Integrated Flight/Propulsion Control System at 3000 m Altitude and 0.5 Mach

The airspeed histories corresponding to each value of the interconnect gains are given in Figure 6. As the interconnect gain is increased, the control law commands lower and lower speeds. The sharp airspeed transitions in Figure 6 are caused due to the simple nature of the interconnect logic. Smoother airspeed transitions can be provided by a more advanced interconnect logic.

The angle of sideslip is maintained close to zero throughout the maneuver, and the angle of attack is chosen to ensure that the vertical component of lift balances with the weight. The angle of attack histories along the turn maneuvers are displayed in Figure 7.



**Fig. 6. Airspeed Histories for the A-4D Aircraft
Integrated Flight/Propulsion Control System ($h = 3000\text{m}$, $M=0.5$)**

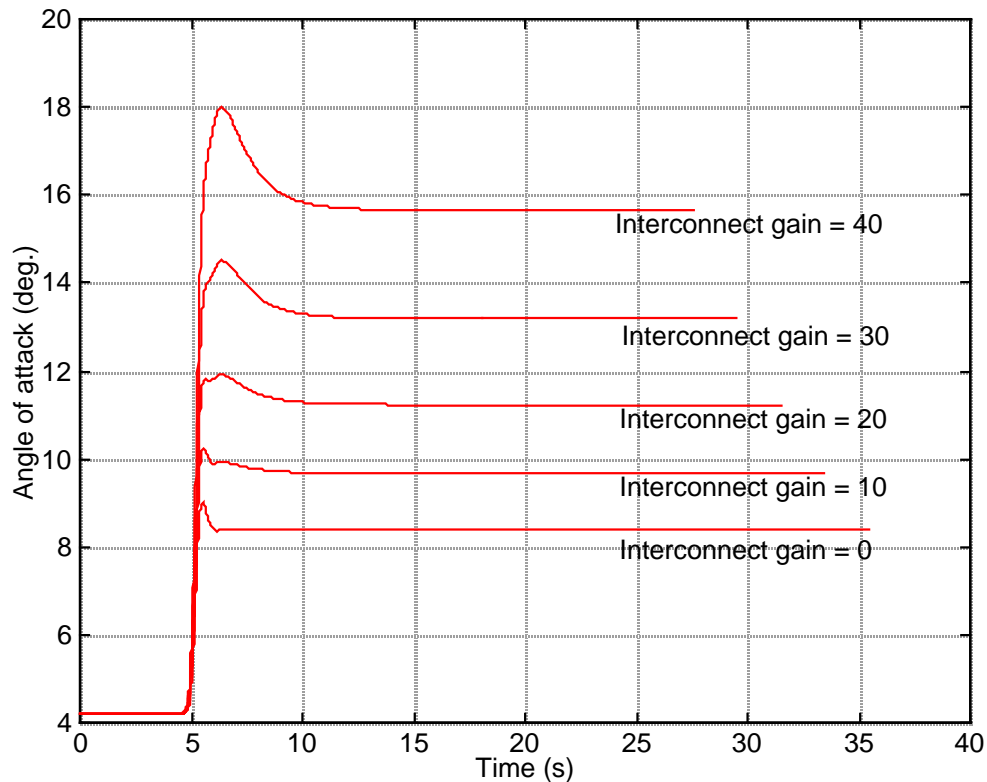


**Fig. 7. Angle of Attack Histories for the A-4D Aircraft
Integrated Flight/Propulsion Control System ($h = 3000\text{m}$, $M=0.5$)**

Note that the aircraft altitude was maintained constant throughout the maneuver in the foregoing simulation. Consequently, as the aircraft speed decreases, higher angles of attack are required to maintain the altitude. Thus, the aircraft stall angle of attack limits the minimum permissible airspeed during the turn. The performance limitations introduced by the stall angle of attack limit can be ameliorated to a certain extent by allowing the aircraft to undergo altitude variations during the turn. For instance, as the aircraft initiates the turn, it can be allowed to increase its altitude thus decreasing the airspeed, and as it comes out of the turn, the speed can be increased to the nominal value by converting some of its potential energy into kinetic energy. However, in that case, a more complex interconnect logic will be required for integrating the flight and propulsion control system. Development of such control laws for flight/propulsion system integration will be a future research item.

The numerical results presented in this section illustrate the benefits of integrating the flight control system with the propulsion system in a conventional high performance aircraft. It is important to observe that every trajectory given in this section corresponds to a load factor of 2 g's. Since turn rate improvements have been realized through a change in control laws, neither

the structural limit nor the pilot endurance limits have to be compromised to achieve the improved performance. This fact has significant practical implications to the flight control system designer.

3. Precision Time Control of A Large Transport Aircraft

As a second application of the integrated flight/propulsion control technology, the problem of precisely controlling the time-of-arrival of a large transport aircraft at specified waypoints is considered in this section. Air traffic control in congested airspace requires each aircraft to follow precise 4-D trajectories in order to ensure adequate inter-aircraft separation. Current generation flight management systems provide limited time-of-arrival capabilities [16], achieved by computing the airspeed along a flight segment based on ambient winds. The constant speed flight segment approach is unlikely to meet the demands of the next generation air traffic management systems [17, 18]. Higher traffic densities anticipated in the next generation air traffic management systems will require a much tighter control over the time of arrival than is currently available. It will be shown in this section that a tight control over the time-of-arrival can be maintained through the use of integrated flight/propulsion control technology.

A longitudinal nonlinear model of the Boeing 747-300 aircraft [9] is employed in this work. The equations of motion describing the longitudinal dynamics of the aircraft are:

$$\begin{aligned}\dot{X} &= a_x - g \sin \theta - qw \\ \dot{w} &= qu + g \cos \theta + a_z \\ \dot{\phi} &= \frac{M}{I_{yy}} \\ \dot{\theta} &= q \\ \dot{h} &= V_T \cos(\theta - \alpha) \\ \dot{X} &= V_T \sin(\theta - \alpha)\end{aligned}$$

In addition to the symbols defined in the previous section, the variable θ denotes the aircraft pitch rate, q is the pitch rate, w is the down ward velocity component in the body axis system, M is the pitching moment, and α is the angle of attack. The symbol h denotes the altitude, V_T is the airspeed and I_{yy} is the aircraft moment of inertia about the aircraft pitch axis. The body acceleration components are given by:

$$a_x = \frac{(\eta T_{\max} - D)}{m} \quad \text{and} \quad a_z = -\frac{L}{m}$$

The lift, drag and pitching moments are computed using the expressions:

$$L = \bar{q}s \left(C_{L_\alpha} \alpha + C_{L_{\dot{\alpha}}} \dot{\alpha} \frac{\bar{c}}{2V_T} + C_{L_q} q \frac{\bar{c}}{2V_T} + C_{L_{\delta_e}} \delta_e \right)$$

$$D = \bar{q}s (C_{D_\alpha} |\alpha|)$$

$$M = \bar{q}s \bar{c} \left(C_{M_\alpha} \alpha + C_{M_{\dot{\alpha}}} \dot{\alpha} \frac{\bar{c}}{2V_T} + C_{M_q} q \frac{\bar{c}}{2V_T} + C_{M_{\delta_e}} \delta_e \right)$$

The aerodynamic coefficients are obtained from Reference [9]. The available thrust data for a version of the Pratt and Whitney JT8D turbofan engine was scaled-up to generate the JT9D-7R4G2 (Boeing 747-300 engine) engine data.

As in the previous section, for the purposes of illustrating the effect of flight/propulsion control system integration, flight control systems similar to those existing on large wide-body aircraft are first designed. In the vertical plane, these consist of the altitude control system and the autothrottle. Next, an interconnect logic is designed to generate altitude/airspeed command perturbations required to achieve precision time control. Due to the preliminary nature of the present study, a simple interconnect logic will be employed here. More advanced integrated flight/propulsion control laws will be examined in a future research effort. Figure 8 illustrates the proposed control system configuration for precision time control.

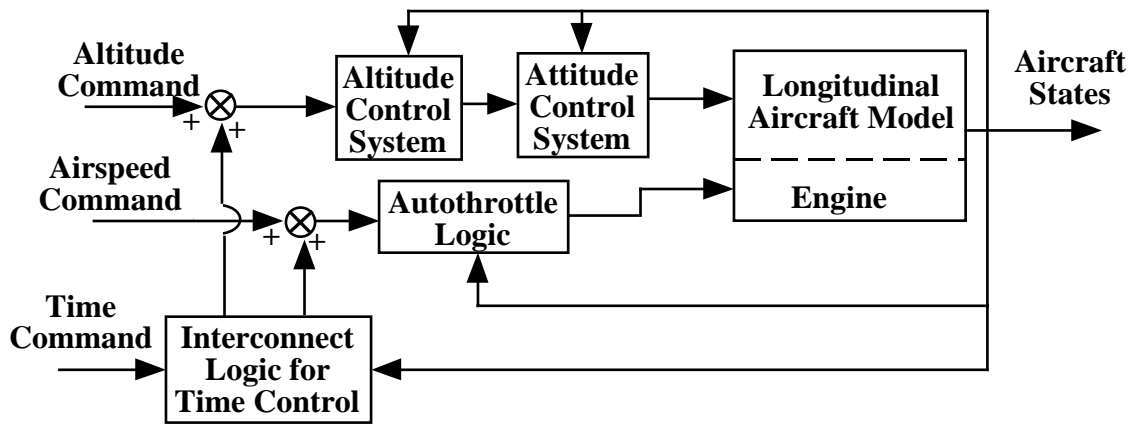


Fig. 8. Integrated Flight/Propulsion Control System for a Large Transport Aircraft

In order to avoid expending any effort in gain scheduling, nonlinear controllers based on feedback linearization will be designed to perform these functions. The first step in the design of altitude control system is the synthesis of a pitch attitude control system. The pitch attitude control system has the responsibility for stabilizing the airframe while tracking the commanded pitch attitude. The altitude tracking control loop is then designed around the pitch attitude control system. The altitude tracking system generates pitch attitude commands in response to altitude errors.

The design of each of these control loops will be discussed in the following. The pitch attitude control system can be designed based on the differential equation for pitch attitude acceleration. This equation can be obtained by differentiating the differential equation for the pitch attitude once with respect to time and substituting for $\dot{\theta}$ to yield:

$$\ddot{\theta} = \frac{\bar{q} s \bar{c}}{I_{yy}} \left(C_{M_\alpha} \alpha + C_{M_{\dot{\alpha}}} \dot{\alpha} \frac{\bar{c}}{2V_T} + C_{M_q} q \frac{\bar{c}}{2V_T} + C_{M_{\delta_e}} \delta_e \right)$$

Setting the right hand side of this equation to a pseudo-control variable U_5 results in a second-order, linear time-invariant linear system. A proportional plus derivative control law can be designed to track commanded pitch attitude θ_c as:

$$U_5 = k_7(\theta_c - \theta) - k_8 \dot{\theta}$$

The elevator deflection δ_e can be recovered by equating this control law to the right hand side of the pitch attitude acceleration equation. Thus,

$$\delta_e = \frac{1}{C_{M_{\delta_e}}} \left[\frac{I_{yy}}{\bar{q} s \bar{c}} \{k_7(\theta_c - \theta) - k_8 \dot{\theta}\} - C_{M_\alpha} \alpha - C_{M_q} q \frac{\bar{c}}{2V_T} - C_{M_{\dot{\alpha}}} \dot{\alpha} \frac{\bar{c}}{2V_T} \right]$$

This expression assumes the availability of the system state variables, and a reasonably accurate aerodynamic model of the aircraft. The feedback gains for the pitch attitude control system can be computed using a specification of the closed-loop system damping and natural frequency. The following values were used for the present work.

$$k_7 = \omega_{n_1}^2, \quad k_8 = 2\zeta_1 \omega_{n_1}, \quad \omega_{n_1} = 6.28 \text{ rad/sec and } \zeta_1 = 0.707$$

Next, an altitude control loop is designed around the attitude control system. The altitude control system uses the expression for vertical acceleration of the aircraft. The differential equation for aircraft altitude acceleration is:

$$\ddot{h} = a_x \sin \theta - a_z \cos \theta - g$$

Setting the right hand side of this expression to a pseudo-control variable U_6 , yields a second-order, linear time-invariant linear system of the form: $\ddot{h} = U_6$

A proportional plus derivative control law can be designed to track commanded altitude profile. Noting that the altitude is controlled by varying the acceleration component a_z , the pseudo-control law can then be equated to the right hand side of the altitude acceleration equation to yield:

$$a_z = \frac{1}{\cos\theta} \left[a_x \sin\theta - k_9(h_c - h) - k_{10}(\dot{h}_c - \dot{h}) - g \right]$$

In conventional aircraft, the acceleration component a_z is altered by changing the angle of attack through the pitch attitude. This fact, together with $\theta = \alpha + \gamma$, and $\gamma = \sin^{-1}\left(\frac{\dot{h}}{V_T}\right)$ can be used to obtain the pitch attitude command required to track a commanded altitude history as:

$$\theta_c = \left\{ k_9(h_c - h) + k_{10}(\dot{h}_c - \dot{h}) - a_x \sin\theta + g \right\} \frac{m}{\bar{q}s \left(C_{L_\alpha} - \frac{C_{L_{\delta_e}}}{C_{M_{\delta_e}}} C_{M_\alpha} \right) \cos\theta} + \sin^{-1}\left(\frac{\dot{h}}{V_T}\right)$$

In the present work, the parameters used for designing the altitude control system are:

$$k_9 = \omega_{n_2}^2, \quad k_{10} = 2\zeta_2\omega_{n_2}, \quad \omega_{n_2} = 0.7854 \text{ rad/sec and } \zeta_2 = 0.707$$

A block diagram of the nonlinear altitude control system is given in Figure 9.

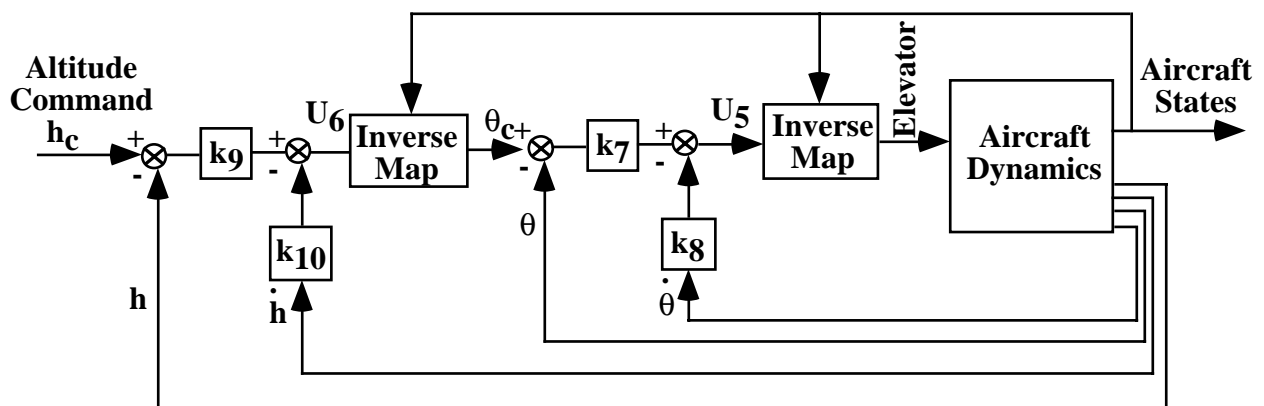


Fig. 9. Altitude Tracking Control System

The airspeed control system (autothrottle) design closely follows the approach presented in the previous section. However, the speed control system in this section is based on the definition of the airspeed $V_T = \sqrt{u^2 + w^2}$. Differentiating this expression once with respect to time yields

$$\dot{V}_T = \frac{u}{V_T} \dot{u} + \frac{w}{V_T} \dot{w} = \frac{u}{V_T} [a_x - g \sin \theta - qw] + \frac{w}{V_T} [qu + g \cos \theta + a_z]$$

As in the previous cases, the right hand side of this expression can be equated to a pseudo-control variable to yield a linear, time-invariant first-order system. Since the system is expected to operate as a regulator, a proportional control law is adequate for the pseudo-control loop. Thus, the autothrottle control logic for the aircraft can be obtained as:

$$\eta = \frac{D}{T_{\max}} + \frac{m}{T_{\max}} \left[\frac{V_T}{u} \left\{ k_{11}(V_{T_c} - V_T) - \frac{w}{V_T} (qu + g \cos \theta + a_z) \right\} + g \sin \theta + qw \right]$$

A block diagram of the airspeed control system is given in Figure 10. The airspeed and altitude control laws can be used to track the commands generated by the air traffic control system.

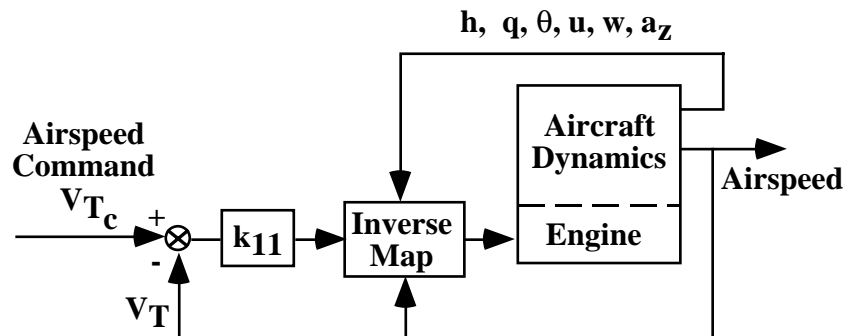


Fig. 10. Airspeed Control System

The air traffic control advisories are generally issued in the form of a series of cruise speed and altitude clearances. As pointed out at the beginning of this section, several flight management systems currently on-board commercial aircraft are capable of meeting required time of arrival (RTA) constraints [16]. They accomplish this function by computing airspeed schedules that would deliver the aircraft at specified waypoints at desired time instants. The speed schedules generated by the flight management system are then executed using the autothrottle system.

However, tracking these speed settings will not result in exactly meeting the time of arrival specifications because the atmospheric conditions may be different from those used in the flight management computations. Meeting precise time specifications will require a closed-loop adjustment of the airspeed as the aircraft follows various altitude/heading advisories. If the aircraft is in climb or in descent, the altitude rate will also have to be adjusted to ensure timely arrival at the specified waypoints. Thus, simultaneous closed-loop control of altitude and airspeed are essential for achieving precision time control.

Precision time control can be achieved by integrating the altitude control system with the speed control system. A simple interconnect logic will be synthesized in the following to demonstrate precision time control through integrated flight/propulsion control technology. The interconnect logic uses the difference between desired time of arrival and the actual time of arrival to determine the incremental altitude and airspeed commands.

The interconnect logic development in the present paper will be based on a “time perturbation” equation. This equation is derived using the down range rate equation:

$$\frac{dx}{dt} = V_T \cos \gamma$$

Rate of change of time with respect to the range is given by:

$$\frac{dt}{dx} = t' = \frac{1}{V_T \cos \gamma}$$

Linearizing this expression yields:

$$\delta t' = -\frac{1}{V_T^2 \cos \gamma} \delta V_T + \frac{1}{V_T \cos^2 \gamma} \sin \gamma \delta \gamma$$

The independent variable in this equation is next changed from range to time by multiplying both sides by the range rate. Next, denoting the nominal values by an under bar, the linearized time rate equation can be written as:

$$\delta \dot{t} = -\frac{1}{\underline{V}_T} \delta V_T + \tan \underline{\gamma} \delta \gamma$$

A few observations can be made regarding this equation. The time rate expression suggests that if the aircraft is in level flight, the flight time can be adjusted only by changing the airspeed. On the other hand, if the aircraft is in climb or descent, the flight time can be adjusted by changing airspeed, and/or the flight path angle. Further, the first term of the expression suggests that a positive airspeed perturbation introduces a negative time rate, i.e., a time delay can be

compensated by using an increase in airspeed and vice-versa. All these observations are consistent with physical intuition.

Only the first term will be included in the present study. In this case, the speed perturbation can be treated as a control variable in the time rate equation. A proportional control law of the form:

$$\delta V_T = k_{12}(t - t_c)$$

can then be used to drive the time errors close to zero. The variable t_c is the desired value of time, and k_{12} is the feedback gain. The airspeed perturbations required to nullify time perturbations can be added to the commanded airspeed to achieve precision time control. Note that in the general case, a combination of altitude rates and airspeed changes will have to be used to correct the time errors.

The autothrottle logic, the altitude control law, together with the interconnect logic are next evaluated using a nonlinear simulation of the aircraft. A nominal wind profile shown in Figure 11 and the Dryden turbulence models [6] were also incorporated in the simulation.

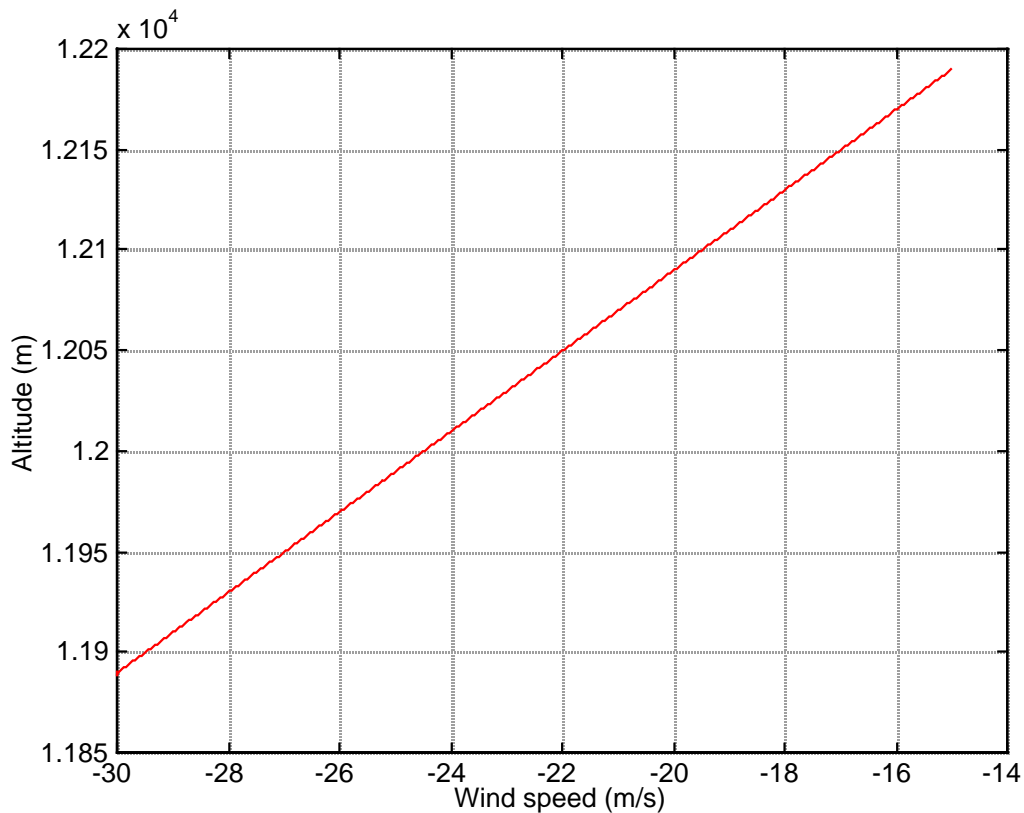


Fig. 11. Nominal Wind Profile Used for Integrated Control Law Evaluation

Performance of the integrated flight propulsion control system in one operational scenario will be illustrated in the following. In this scenario, the aircraft is initially in level flight at 11890 m altitude, at 0.74 Mach. At about 4 km down range, the aircraft is required to climb to 12190 m while increasing its speed to 0.78 Mach at about 11 km down range. The simulation is terminated at 14 km down range.

The time of arrival at 14 km range without including any wind or gust disturbances is considered to be the required time of arrival. It can be observed from Figure 11 that the aircraft has to traverse a head-wind profile that varies with altitude. Thus, in the present simulation, the effect of the wind is to delay the aircraft with respect to the nominal arrival time.

The altitude tracking performance of the flight control system is given in Figure 12. The solid line in this figure corresponds to the altitude command history, while the broken line denotes the actual altitude profile. It can be observed that the system has a finite steady state error while tracking a ramp altitude command. If desired, this error can be compensated using an integral feedback in the altitude channel. This was not done due to the preliminary nature of the present study.

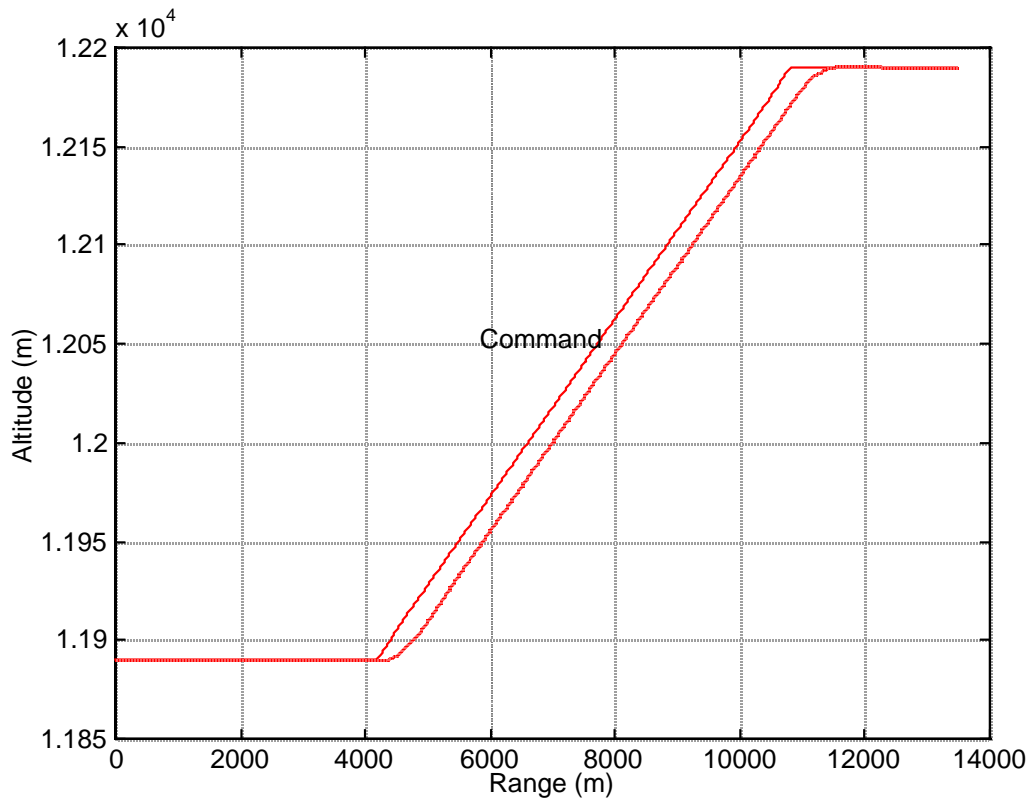


Fig. 12. Commanded and Actual Altitude histories

The time error histories for various values of the interconnect gain k_{12} are shown in Figure 13. Without the interconnect logic, the aircraft arrives at the 14 km waypoint with almost 7 seconds time delay, corresponding to about 10% of the flight time in the present simulation. The time delay is reduced to a fraction of a second using the interconnect logic. More sophisticated interconnect logics will be able to further decrease the time error.

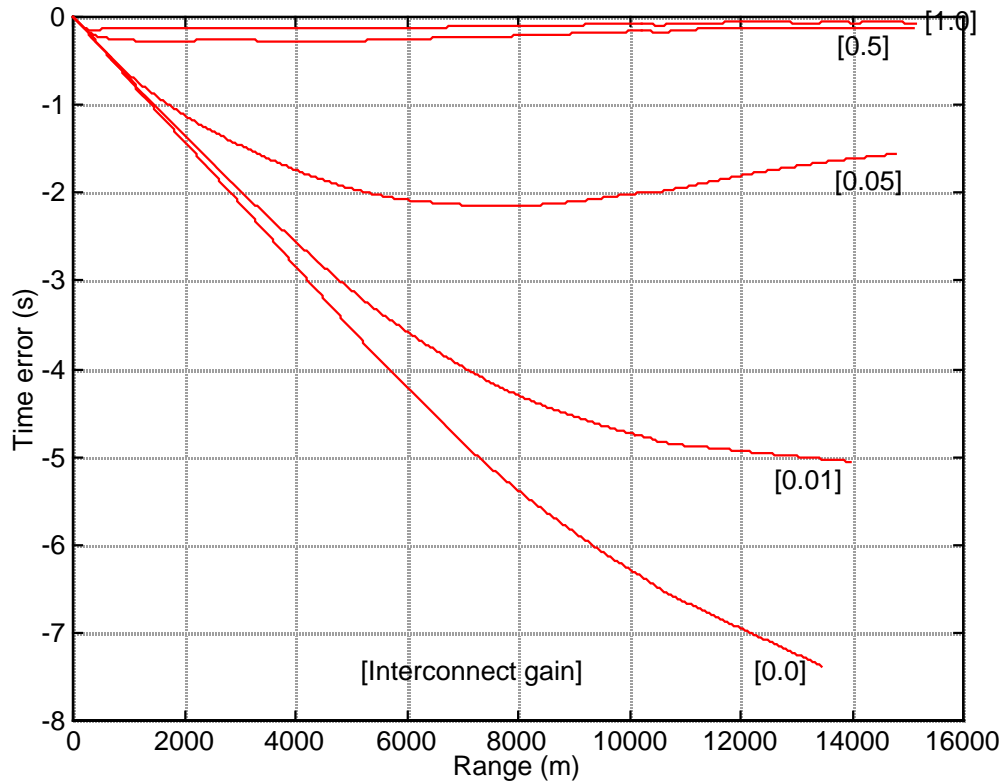


Fig. 13. Time Error With and Without the Interconnect Logic

The airspeed histories corresponding to various interconnect gains are shown given in Figure 14. Unlike the conventional constant speed flight segment case, the airspeed history is continuously adjusted to compensate for the time delay as the aircraft follows the prescribed flight path. It may be observed that the autothrottle system has a significant response to the gusts, as can be observed in Figure 14.

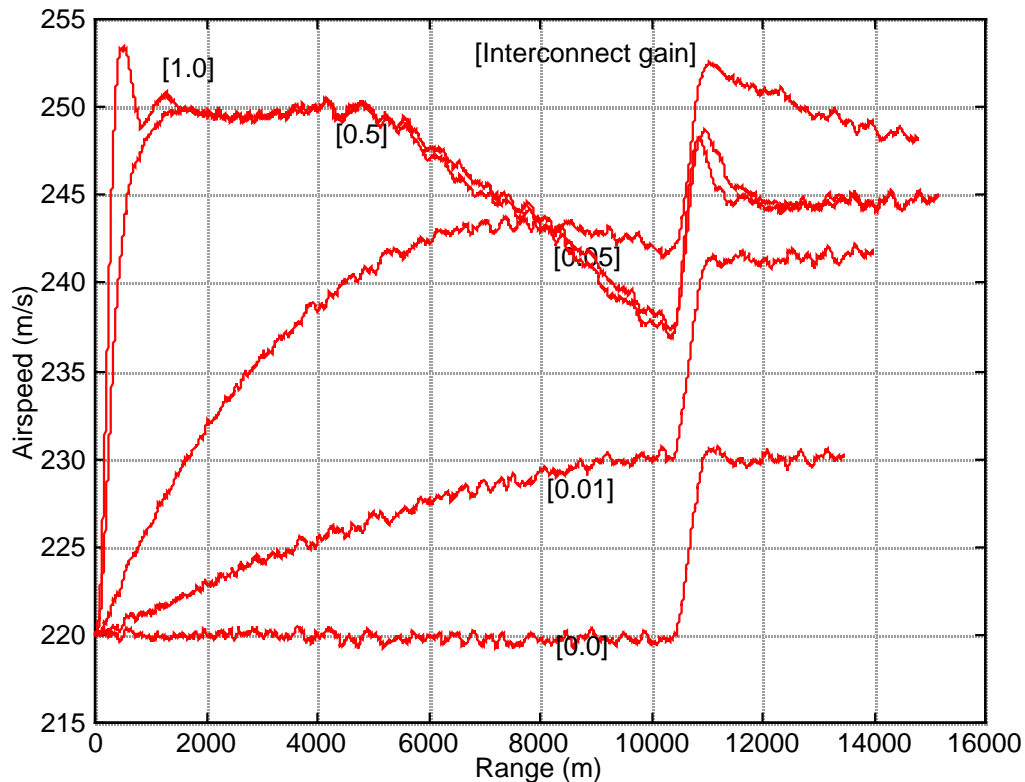


Fig. 14. Airspeed Histories With and Without the Interconnect Logic

The simulation results presented in this section demonstrate the potential improvements in time-of-arrival accuracy possible through integrated flight/propulsion control. Given that most large commercial aircraft already have altitude control and autothrottle systems on-board, the proposed precision time control algorithm can be implemented with relative small incremental cost. The consequent improvements in the air traffic control environment will be valuable for improving flight safety.

Conclusions

In this paper the benefits of integrating the propulsion system with the primary flight control system in conventional aircraft was explored using two different examples. In the first example, it is shown that the aircraft turn rate at a specified load factor can be improved by modulating the airspeed during the turn using an integrated flight/propulsion control system. The second example considered precision time control of a large transport aircraft in a modern air traffic control environment. In these aircraft, on-board flight management systems can be used to achieve a required time-of-arrival in the range of 10 to 30 seconds. The uncertainty in the time-of-arrival is caused largely by the wind and temperature variations, and cannot be precisely

compensated for using open-loop estimation of wind speed. It is shown that by integrating the propulsion system control to the primary flight control, the time of arrival at specified waypoints can be regulated with a high accuracy. This capability will be valuable in the next generation air traffic automation systems.

Acknowledgment

This research was supported by NASA Lewis Research Center under contract NAS3-27578, with Dr. Sanjay Garg serving as the Technical Monitor.

References

- [1] Garg, S. and Schmidt, P. H., "Application of Controller Partitioning Optimization Procedure to Integrated Flight/Propulsion Control Design for a STOVL Aircraft", *1993 AIAA Guidance, Navigation, and Control Conference*, Aug. 9 -11, 1993, Monterey, CA.
- [2] Garg, S., "Robust Integrated Flight/Propulsion Control Design for a STOVL Aircraft using H-Infinity Control Design Techniques", *Automatica*, Vol. 29, No. 1, pp. 129-145, 1993.
- [3] Garg, S., and Mattern, D. L., "Application of Integrated Flight/Propulsion Control Design for a STOVL Aircraft", *1991 AIAA Guidance, Navigation, Control Conference*, New Orleans, LA, Aug. 1991.
- [4] Schierman, J., Schmidt, D. K., Lovell, T., "Analysis of Airframe/Engine Interactions for a STOVL Aircraft with Integrated Flight/Propulsion Control", *AIAA Guidance, Navigation, and Control Conference*, Hilton Head, SC, August 1991.
- [5] Schmidt, D. K., "Integrated Control of Hypersonic Vehicles - A Necessity Not just a Possibility", *1993 AIAA Guidance, Navigation, and Control Conference*, Aug. 9 -11, 1993, Monterey, CA.
- [6] McLean, D., *Automatic Flight Control Systems*, Prentice-Hall, New York, NY, 1990.
- [7] Kelley, H. J., Aircraft Maneuver Optimization through Reduced-Order Approximation, in *Control and Dynamic Systems Vol. 10*, Edited by C. T. Leondes, Academic Press, New York, 1973, pp. 131-178.
- [8] Well, K. H., Farber, B., and Berger, E., "Optimization of Tactical Aircraft Maneuvers Utilizing High Angles of Attack", *Journal of Guidance and Control*, Vol. 5, March-April 1982, pp. 131-137.
- [9] Nelson, R. C., *Flight Stability and Automatic Control*, McGraw-Hill, New York, NY, 1989.

- [10] Gunston, W., and Spick, M., *Modern Air Combat*, Crescent Books, New York, 1983.
- [11] Menon, P. K., “Optimal Symmetric Flight with and Intermediate Model”, *Ph. D Dissertation*, Virginia Polytechnic Institute and State University, 1983.
- [12] Menon, P. K., Badgett, M. E., Walker, R. A., and Duke, E. L., “Nonlinear Flight Test Trajectory Controllers for Aircraft”, *Journal of Guidance, Control, and Dynamics*, Vol. 10, Jan.-Feb.. 1987, pp. 67-72.
- [13] Isidori, A., *Nonlinear Control Systems - An Introduction*, Springer-Verlag, New York, 1989.
- [14] Meyer, G., and Cicolani, L., “Application of Nonlinear Inverses to Automatic Flight Control Design-System Concepts and Flight Evaluations”, AGARDograph 251 on *Theory and Applications of Optimal Control in Aerospace Systems*, 1980.
- [15] Menon, P. K., “Nonlinear Command Augmentation System for a High Performance Aircraft”, *1993 AIAA Guidance, Navigation, and Control Conference*, Aug. 9 -11, 1993, Monterey, CA.
- [16] Fadden, D. M., and Schwab, R. W., “Aircraft Interface with Future ATC System”, *Proceedings of the IEEE*, November 1989, pp. 1745 - 1751.
- [17] Erzberger, H., and Nedell, W., “Design of Automated System for Management of Arrival Traffic”, NASA TM 102201, June 1989.
- [18] Davis, T. J., Erzberger, H., and Green, S., “Design and Evaluation of an Air Traffic Control Final Approach Spacing Tool”, *Journal of Guidance, Control, and Dynamics*, Vol. 14, No. 4, July-Aug. 1991, pp. 848 - 854.